Received: 7 May 2020 | Revised: 20 October 2020 | Accepted: 26 October 2020 | Published on: 9 November 2020

DOI: 10.1002/joc.6910

RESEARCH ARTICLE

International Journal of Climatology RMetS

Towards broad-scale temperature reconstructions for Eastern North America using blue light intensity from tree rings

Grant L. Harley[1] | **Karen J. Heeter**[1] | **Justin T. Maxwell**[2] | **Shelly A. Rayback**[3] | **R. Stockton Maxwell**[4] | **Ty E. P. Reinemann**[1] | **Alan H. Taylor**[5]

[1]Department of Geography and Geological Sciences, University of Idaho, Moscow, Idaho

[2]Department of Geography, Indiana University, Bloomington, Indiana

[3]Department of Geography, University of Vermont, Burlington, Vermont

[4]Department of Geospatial Science, Radford University, Radford, Virginia

[5]Department of Geography, Pennsylvania State University, University Park, Pennsylvania

Correspondence
Grant L. Harley, Department of Geography and Geological Sciences, University of Idaho, Moscow, Idaho, 83844, USA.
Email: gharley@uidaho.edu

Funding information
Division of Atmospheric and Geospace Sciences, Grant/Award Numbers: AGS-1805276, AGS-2002524; Division of Behavioral and Cognitive Sciences, Grant/Award Number: BCS-1229887; US National Science Foundation Paleo Perspectives on Climate Change program

Abstract

Summer temperatures across eastern North America (hereafter East) will soon reach a level consistently above any observation experienced during the instrumental period. Increasing temperatures will have negative impacts on natural (e.g., water, plant and animal communities) and human (e.g., health, infrastructure, economies) systems upon which the large and growing centres of human population across the region depend. Within the network of Northern Hemisphere tree-ring temperature proxy records, one of the most obvious geographic holes is the East, where few temperature-sensitive proxies exist. Here we present the first steps towards building a network of temperature-sensitive proxy records across the East using blue light intensity (BI) methods applied to the tree rings of multiple temperature sensitive tree species situated from North Carolina to Maine, USA. Our overall objective is to report on the most viable species for BI analysis across different regions of the East (e.g., Southeast US, Midwest US, Northeast US/Canadian Maritimes) by exploring temporal (e.g., since ca. 1900) and spatial relationships between instrumental temperatures and BI metrics. We found BI to be a strong predictor of March–October mean air temperature ($R^2 = 0.61$) across the Northeast US/eastern Canada, and Sep-Oct maximum air temperature ($R^2 = 0.42$) across the Southeast US. Of all species tested, *Tsuga canadensis* and *Picea rubens* contained the strongest BI temperature signal. Adding more BI sites from these and potentially other species, as well as inclusion of other temperature proxies (e.g., ring widths) will allow for the development of a skilful broad-scale and long-term temperature field reconstruction across the East.

KEYWORDS

blue light intensity, climate change, dendrochronology, northern hemisphere temperature, *Picea rubens*, *Tsuga canadensis*

Equally contributing authors.

1 | INTRODUCTION

Summer temperatures across eastern North America (hereafter East) increased by more than 1°C during the 20th century. Current and future increasing temperatures will have negative impacts on natural (e.g., water, plant and animal communities) and human (e.g., health, infrastructure, economies) systems. More accurate predictions of summer temperatures across the East require better understandings of historic variability. The last two decades have seen a considerable amount of effort directed towards developing a network of high-resolution temperature proxy records across the Northern Hemisphere. As part of this effort, most studies were focused on using tree rings as a proxy for temperature variability (e.g., Esper *et al*., 2002; Frank *et al*., 2007; Wilson *et al*., 2007), but other studies included multiple proxy records in addition to tree rings (e.g., Jones *et al*., 1998; Mann *et al*., 1999; Wahl and Ammann, 2007; Mann *et al*., 2009). Yet, within the network of Northern Hemisphere tree-ring temperature proxy records, one of the most obvious geographic gaps occurs in the East USA, where few to no temperature reconstructions exist. Longer temperature records for the East will provide information on (a) the full range and amplitude of pre-instrumental temperatures, (b) past and current spatiotemporal characteristics of temperature variability, (c) the timing, trends, and duration of temperature rate changes, and (d) the influence of broad-scale ocean and atmosphere forcing mechanisms on pre-instrumental temperatures. Yet, before robust reconstruction models are developed, viable temperature proxies must be identified and validated.

Since the 1970s, X-ray-based measurement techniques have been used to produce tree-ring parameters, such as maximum latewood density (MXD), that have been the standard when it comes as extracting a temperature signal from tree rings (Björklund *et al*., 2019). In North America, tree-ring derived temperature reconstructions have been restricted to higher latitude areas, where temperature is expected to be the most limiting factor on tree growth (Jacoby and D'Arrigo, 1989; Briffa *et al*., 1992; Briffa *et al*., 2001; Anchukaitis *et al*., 2013). Throughout the late 1980s and 1990s, increased efforts were placed on developing networks comprised of both MXD and RW chronologies for summer temperature reconstructions across increasingly larger spatial extents (Briffa *et al*., 1988; Briffa *et al*., 1992; Schweingruber *et al*., 1993; Schweingruber and Briffa, 1996; Trouet and Van Oldenborgh, 2013). As an affordable surrogate to X-ray-based MXD, reflected visible light-based techniques have become increasingly popular over the past decade (Campbell *et al*., 2007). Blue light intensity (BI) methods use reflected light in the blue wavelengths from carefully prepared wood surfaces, where denser wood reflects less light. The continuous use of BI metrics, such as inverted latewood BI (LWB) and ΔBI (the difference between EWB and LWB; hereafter DBI), have made it obvious that BI is intimately linked to MXD, and is therefore increasingly adopted into the field of dendroclimatology (McCarroll *et al*., 2002; Björklund *et al*., 2014; Rydval *et al*., 2014; Wilson *et al*., 2014; Dolgova, 2016). Despite these advantages over MXD, to date, most BI studies are restricted geographically to high-latitude areas (Luckman *et al*., 1997; Wilson and Luckman, 2003; Wilson *et al*., 2016; Björklund *et al*., 2019). Heeter *et al*. (2019) demonstrate the first successful application of BI in the East for the purposes of (a) determining the efficacy of using BI as a temperature proxy on a low-latitude population of red spruce (*Picea rubens* Sarg.) and (b) assessing the influence of disturbance (e.g., insect outbreak, logging) on BI results. They measured BI on red spruce increment cores—collected previously by White *et al*. (2012)—from a red spruce-Fraser fir *Abies fraseri* (Pursh) Poir. habitat on Roan Mountain, North Carolina that had clear evidence of early 20th century logging and widespread infestation of balsam woolly adelgid (*Adelges piceae* Ratz.). While White *et al*. (2012) showed a negative response in ring-width to disturbance events, Heeter *et al*. (2019) demonstrated that BI methods can be used skilfully on a high-elevation (ca. 2000 m above sea level; masl), lower-latitude (ca. 36°N), and heavily-disturbed population of red spruce. While ring-width response of red spruce showed a drastic decline in response to temperature since 1950, the BI retained a highly correlated ($r = .62$, $p < .001$) and stable response to September–October maximum monthly temperature during the period 1950–2008.

In this paper, we build on the findings of Heeter *et al*. (2019) and discuss the potential for building a broad-scale BI network that could provide multi-centennial temperature reconstructions from a wide variety of species distributed across the East. Our overall objective is to report on the most viable species for BI analysis across different regions of the East (e.g., Southeast US, Midwest US, Northeast US/Canadian Maritimes) by identifying temporal (e.g., since ca. 1900) and spatial relationships between instrumental temperature records and BI metrics. The species we selected were long-lived, temperate conifers that could have potential for developing multi-century temperature reconstructions and include red spruce, eastern hemlock (*Tsuga canadensis* L.), Carolina hemlock (*Tsuga caroliniana* Engelm.), and Fraser fir.

2 | MATERIALS AND METHODS

2.1 | Ring-width and BI data

For this study, we added more samples to the Roan Mountain collection detailed in Heeter *et al*. (2019), as well as sampled increment cores from additional sites—4 red spruce, 1 Carolina hemlock, and 1 eastern hemlock—across the southern Appalachian Mountain region of North Carolina, USA during May 2019. We also acquired tree-ring samples collected previously across the Southeast, Midwest, and Northeast US regions, including 1 Fraser fir from North Carolina, 1 red spruce from Vermont, and total of 8 eastern hemlock from Indiana (2), Ohio (1), Maine (4), and Connecticut (1) (Table 1; Figure 1).

At each site, 20–40 living trees were sampled with a 5 mm increment borer, taking two cores per tree. In the laboratory, samples exhibiting discolorations were immersed in acetone (99.5%) for approximately 72 hours to remove as much resin content and pigmentation as possible, then resurfaced to a high polish (e.g., 600 grit sandpaper; Speer, 2010). All cores were then scanned at 3200 dpi using an Epson 12000XL scanner, calibrated using an IT8.7/2 calibration card coupled with 8.9 Silverfast software. We then measured all cores to the 0.001 precision in CooRecorder (Larsson, 2014). After visual crossdating of all cores, we used the computer program COFECHA (Holmes, 1983) to statistically compare measurement series for crossdating and ensure measurement accuracy. After cores were absolutely dated and measured, we obtained measurements of ring width and BI (e.g., LWB or DBI) for each core using CooRecorder. Using the SignalFree (SF) program (Melvin and Briffa, 2008), both ring-width and BI measurements were standardized with an age-dependent spline (ADSsf) (sensu Wilson *et al*., 2019; Heeter *et al*., 2019) and combined into site-specific chronologies using a bi-weight average. We assessed the homogeneity of the inter-site chronology signal within each region using principal component analysis (PCA) over the common period, which differed depending on the region. Last, we examined geographic characteristics (e.g., elevation, latitude) of individual chronology loading strengths to the first principal component (PC_1).

TABLE 1 Blue intensity chronology site locations and information included in this study

Site	Species	State	Lat °N	Long °W	m.a.s.l.	# cores(trees)	Period
			Northeast				
Mattawaumkeag	*T. canadensis*	Maine	45.50	−68.28	102	37(16)	1787–2012
Boody pond	*T. canadensis*	Maine	44.56	−69.95	289	38(20)	1899–2012
Little concord pond	*T. canadensis*	Maine	44.44	−70.54	372	40(19)	1,681–2012
Bradbury	*T. canadensis*	Maine	43.89	−70.18	157	40(21)	1896–2012
Cape NRA	*P. rubens*	Vermont	43.48	−72.59	659	38(20)	1811–2009
Bigelow pond	*T. canadensis*	Connecticut	41.95	−73.22	283	59(17)	1700–2012
			Midwest				
Cliff forge	*T. canadensis*	Ohio	40.60	−82.29	302	38(20)	1868–2016
Pine Hills	*T. canadensis*	Indiana	39.94	−87.05	216	12(9)	1817–2014
Liar's bench	*T. canadensis*	Indiana	39.21	−86.24	181	27(18)	1914–2013
			Southeast				
Roan Mtn	*P. rubens*	North Carolina	36.11	−82.04	1916	38(20)	1874–2008
Roan Mtn	*A. fraseri*	North Carolina	36.11	−82.04	1916	40(20)	1935–2008
Mt Mitchell	*P. rubens*	North Carolina	35.77	−82.26	1976	38(20)	1819–2018
Mt Collins	*P. rubens*	North Carolina	35.59	−83.47	1883	42(20)	1681–2018
Clingman's dome	*P. rubens*	North Carolina	35.56	−83.49	2022	40(20)	1788–2018
Alarka	*P. rubens*	North Carolina	35.34	−83.35	1260	40(20)	1889–2018
Kelsey tract	*T. caroliniana*	North Carolina	35.08	−83.18	1275	40(20)	1884–2018
Kelsey tract	*T. canadensis*	North Carolina	35.08	−83.18	1275	40(20)	1723–2018

Note: m.a.s.l. = meters above sea level (elevation); Species = *Tsuga canadensis* (eastern hemlock), *Tsuga carolinana* (Carolina hemlock), *Picea rubens* (red spruce), *Abies fraseri* (Fraser fir).

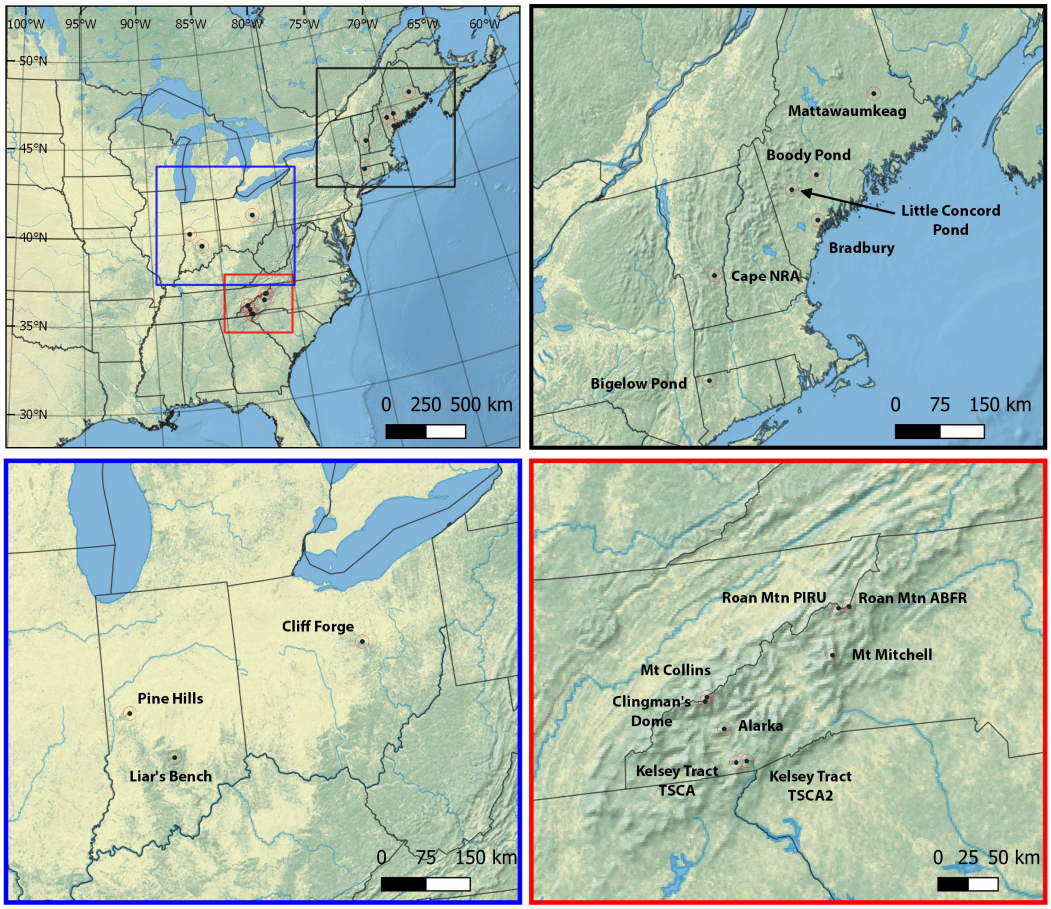

FIGURE 1 Study area map of the current eastern North America blue intensity network. Locations of study sites across the three study regions, Northeast (black), Midwest (blue), and Southeast (red)

2.2 | Ring width and BI relationships with temperature

We used Pearson correlation analysis to test temporal relationships between individual site RW and BI metrics and temperature data using the TreeClim package in R (Zang and Biondi, 2015). Next, spatial field correlations were performed between each chronology and gridded temperature data (e.g., monthly maximum and mean temperature (T_{max}; T_{mean}) from the CRU TS v4.03 data set (Harris *et al.*, 2013) averaged over the three regions of interest: Northeast, Midwest, and Southeast. We used the CRU data set, as opposed to PRISM (Daly *et al.*, 2008), as it extends into Canada and allows us to better asses regional spatial patterns between BI and temperature. We also assessed the relationships between temperature and a regional composite time series, represented by PC_1 for each region. We calculated correlations over the entire available instrumental period 1895–2018, but the length of analysis depended on the length of each chronology.

We also examined the temporal stability of the BI temperature signal across the tested regions. In the R package "dlm" (Petris, 2010), we used a state-space model with time-varying parameter regression and the Kalman filter to test for signal stability between BI metrics and temperature over the instrumental period (Kalman, 1960; Durbin and Koopman, 2012). In our case of applying the Kalman filter to BI-temperature relationships, the assumption that BI is constantly determined by temperature is relaxed, which allows the detection of changes in the relationships. This method is used commonly to detect temporal changes in the relationships between tree-ring parameters (i.e., ring width) and climate over time (Cook and Johnson, 1989; Visser *et al.*, 2010; Bishop *et al.*, 2015; Maxwell *et al.*, 2019).

3 | RESULTS AND DISCUSSION

3.1 | RW and BI data

Across the Northeast region, we compared RW and BI data at 6 sites: 5 eastern hemlock and 1 red spruce. The eastern hemlock and red spruce increment cores did not

TABLE 2 Interseries correlation (RBAR) and number of series needed for a strong shared signal (EPS > 0.80) for the Northeast LWB chronologies. RBAR and EPS calculated using ADSsf detrending

Site	RW RBAR	RW no. series EPS	RW year EPS	LWB RBAR	LWB no. series EPS	LWB year EPS
Mattawaumkeag	0.54	1	1799	0.33	10	1886
Boody Pond	0.35	3	1899	0.20	18	1924
Little Concord Pond	0.41	7	1806	0.22	16	1898
Bradbury	0.39	4	1901	0.23	19	1925
Cape NRA	0.29	8	1872	0.24	14	1903
Bigelow Pond	0.49	6	1770	0.34	9	1785

Note: RBAR = mean interseries correlation; No. series EPS = the number of measured series to carry EPS > 0.80. Year EPS = the year EPS drops < 0.80.

TABLE 3 RBAR and number of series needed for a strong shared signal (EPS > 0.80) for the Midwest LWB chronologies. RBAR and EPS calculated using ADSsf detrending

Site	RW RBAR	RW no. series EPS	RW year EPS	LWB RBAR	LWB no. series EPS	LWB year EPS
Pine Hills	0.38	4	1823	0.36	12	1890
Liar's Bench	0.45	6	1950	0.41	14	1958
Cliff Forge	0.38	7	1917	0.25	11	1936

Note: RBAR = mean interseries correlation, No. series EPS = the number of measured series to carry EPS > 0.80; Year EPS = the year EPS drops <0.80.

TABLE 4 RBAR and number of series needed for a strong shared signal (EPS > 0.80) for the Southeast LWB chronologies. RBAR and EPS calculated using ADSsf detrending

Site	RW RBAR	RW no. series EPS	RW year EPS	DBI RBAR	DBI no. series EPS	DBI year EPS
Roan Mtn PIRU	0.31	3	1891	0.26	6	1912
Roan Mtn ABFR	0.37	6	1941	0.21	14	1946
Mt Collins	0.33	10	1805	0.44	12	1818
Clingman's Dome	0.36	6	1851	0.27	10	1899
Mt Mitchell	0.35	2	1893	0.27	11	1942
Alarka	0.39	12	1924	0.27	13	1925
Kelsey Tract TSCA	0.55	6	1812	0.46	7	1822
Kelsey Tract TSCA2	0.47	6	1898	0.38	9	1900

Note: RBAR = mean interseries correlation; No. series EPS = the number of measured series to carry EPS > 0.80; Year EPS = the year EPS drops <0.80; PIRU = *Picea rubens* (red spruce); ABFR = *Abies fraseri* (Fraser fir); TSCA = *Tsuga canadensis* (eastern hemlock); TSCA2 = *Tsuga carolinana* (Carolina hemlock).

demonstrate noticeable colour changes from heartwood to sapwood, or high resin content. Thus, we measured LWB rather than DBI. Sites were located from 45.5°N south to 41.9°N, and spanned longitudinally from northwestern Connecticut (−73.2°W) to the Mattawaumkeag site in east-central Maine (−68.3°W), which served to be the northernmost site as well (Table 1; Figure 1). Site elevations ranged 102–659 masl. The longest record was Little Concord Pond, spanning the period 1681–2012, and the shortest record was Boody Pond (1899–2012). All RW and LWB eastern hemlock chronologies spanned the instrumental period from 1900 to 2012, but the outermost year of the Cape NRA red spruce collection was 2009. Agreement between measured series (e.g., mean interseries correlation, RBAR) was stronger for RW compared to LWB at each site (Table 2). Further, LWB chronologies required more than twice as many series to achieve an EPS > 0.80, except at Bigelow Pond. Bigelow showed the highest LWB RBAR (0.34) and fewest number of measured series (n = 9) to achieve a high EPS. Finding a stronger common signal between RW measurements compared to BI metrics was not unexpected, as this has been shown by previous studies (Rydval *et al*., 2014; Wilson *et al*., 2017a; Wilson *et al*., 2017b; Heeter *et al*., 2019; Wilson *et al*., 2019). Recently, Wilson *et al*. (2019) showed that, for white spruce (*Picea glauca* [Moench] Voss) sites

from the southern Yukon, RBAR ranged 0.21–0.47 for RW and 0.10–0.23 for LWB. For the Northeast LWB sites, RBAR range for RW was 0.29–0.54 and 0.20–0.34 for LWB, which was comparable to Yukon measurements.

The three eastern hemlock sites in the Midwest region spanned various time periods, with outermost years ranging from 2013 to 2016 (Table 3). Although the spatial distribution of the Midwest sites was more limited compared to the Northeast, the 3 eastern hemlock sites derive from small, disjunct populations along the western geographical range margin for the species in North America. The northern- and easternmost most site was Cliff Forge (40.6°N, −82.3°W), which spanned the period 1868–2016. The southernmost site, Liar's Bench, was located at 39.2°N, and the westernmost site, Pine Hills, was located at −87.05°W. Site elevations ranged from 181 to 302 masl. As in the Northeast, the 3 Midwest sites demonstrated stronger RBAR for RW compared to LWB. RBAR for RW ranged 0.38–0.45 and 0.25–0.41 for LWB, slightly higher than numbers for the Northeast sites. Of all chronologies included in this study, Liar's Bench was the youngest, having only extended to 1958 with EPS > 0.80. Only one chronology, Pine Hills, extended beyond the full length of the instrumental period for subsequent climate analyses. Cliff Forge included the highest sample depth (38 cores from 20 trees) of all Midwest sites, yet demonstrated the lowest LWB RBAR.

We compared a total of 8 sites from 4 different species across the Southeast region. Unlike the Cape NRA red spruce site in the Northeast, the red spruce cores collected from the Southeast demonstrated visible coloration differences between heartwood and sapwood, even after acetone treatments, as did the Carolina hemlock collection from Kelsey Tract. Therefore, we measured DBI rather than LWB, as LWB showed a noticeable step changes or shifts in BI values later in the measured series. The shortest site DBI chronology, based on EPS, was the Fraser fir collection from Roan Mtn (1946–2008) (Table 4). The Southeast site locations followed a northeast-southwest trajectory along the upper-elevations of the Southern Blue Ridge Mountains. Elevations ranged from Alarka at 1260 masl up to Clingman's Dome at 2022 masl. The spatial distribution of sites was also limited compared to the Northeast. However, this region represents the southern range margin for the two primary species included in this study, eastern hemlock and red spruce. Roan Mtn was the northernmost and easternmost Southeast site location at 36.1°N, −82.0°W. The southernmost site was the Kelsey Tract at 35.0°N.

Agreement between measured series for RW outperformed DBI for all sites except one: Mt. Collins. RW RBAR ranged 0.31 to 0.55, and 0.21 to 0.46 for DBI. As with the other regions, the DBI metric required more samples to carry a strong common signal, but the differences between RW and DBI with regard to the number of series required to carry an EPS > 0.80 was smaller in the Northeast. Two of the Southeast sites, Roan Mtn and Kelsey Tract, offered a comparison of multiple, co-occurring species. At Roan Mt, although Fraser fir RW was stronger than red spruce, red spruce DBI was stronger than Fraser fir. Out of all sites, the Roan Mtn red spruce required the least amount of samples to carry a strong EPS. At the Kelsey Tract site, eastern hemlock was stronger for both RW and DBI compared to Carolina hemlock.

3.2 | Climate response

Across the Northeast, we identified strong and positive relationships between individual LWB site chronologies and mean Mar-Oct temperature (T_{mean}) during the instrumental period (1900–2009/2012). Correlations between each LWB chronology and T_{max} also showed strong and significant results, though slightly weaker; thus we proceeded with T_{mean}. We tested monthly (previous Apr-current Oct) correlations for each site, and temperatures averaged over the Mar-Oct time period were consistent in producing the strongest temporal and spatial relationships. Due to the increasing trend in monthly instrumental T_{mean} data, we tested correlations using nontransformed (raw) and first differenced data. Figure S1 shows monthly correlation analysis between nontransformed (A) and first differenced (B) previous April to current October T_{mean} and PC_1 of RW and LWB, as well as averaged Mar-Oct, during the period 1900–2012. While the highest single-month correlations for LWB were for current Aug (r = .65), every month tested returned significant positive results except previous Oct and current Jan. Averaged T_{mean} data during the Mar-Oct season was the strongest season (r = .78) for both raw and first differenced data. We also tested maximum temperatures (T_{max}) against each LWB site chronology. Both temporal and spatial relationships between T_{mean} and T_{max} were similar, but slightly stronger for T_{mean} for each site. For that reason, we only display results from T_{mean}.

In the East, ring widths from a limited number of tree species are known to exhibit sensitivity to temperature: *Chamaecyparis thyoides* L. (Atlantic white cedar; AWC), eastern hemlock, and red spruce. AWC exhibits a prior- and current-year winter, spring, and summer temperature signal (Pederson *et al*., 2004; Hopton and Pederson, 2005). Pearl *et al*. (2017) used a network of AWC tree-ring width chronologies from New England to develop a mean Jan-Aug temperature reconstruction that

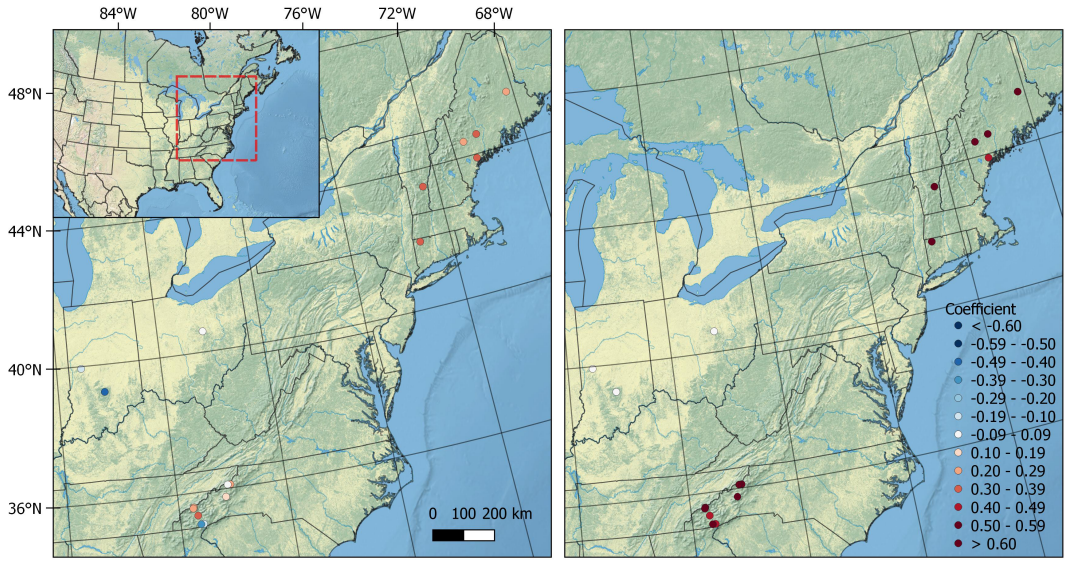

FIGURE 2 Ring width (RW; left)/BI (right)-temperature relationship maps for the eastern North America network regions of the Northeast (NE), Midwest (MW), and Southeast (SE). Left map shows individual site correlation coefficients between RW and the highest-correlated mean (NE,MW) and max (SE) seasonal temperatures for the NE, MW, and SE regions (Mar-Oct; June-Aug; Sep-Oct, resp.) during the period of analysis (1900–2009/2012, 1900–2013,2014,2016; 1950–2008/2018, resp.). Right map shows individual site correlation coefficients between LWB (NE,MW) and DBI (SE) and the highest-correlated mean (NE,MW) and max (SE) seasonal temperatures for the NE, MW, and SE regions (Mar-Oct; June-Aug; Sep-Oct, resp.) during the period of analysis (1900–2009/2012, 1900–2013,2014,2016; 1950–2008/2018, respectively)

extended back to 1860 and explained 34% of the instrumental variance. In a follow-up paper, Pearl *et al.* (2020) used an expanded AWC tree-ring width network to produce a temperature (Jan-Aug) field reconstruction for New England, as well as precipitation and drought reconstructions for the coastal New England and Cape Cod, MA region. Considered a cove species, eastern hemlock—an evergreen, shade-tolerant, long-lived (>400 years), and broadly-distributed conifer in the East that grows in mesic, cove habitats (Burns *et al.*, 1990—has been shown to contain a prior-year temperature signal (Cook and Cole, 1991; Tardif *et al.*, 2001; Saladyga and Maxwell, 2015). The typical climate response of eastern hemlock ring-width chronologies tends to be a signal of positive response to summer moisture availability coupled with a negative response to summer temperatures (e.g., classic moisture availability climate signal; Fritts, 1976), while also showing significant positive responses to spring temperatures, primarily during the month of March (Cook and Cole, 1991; D'Arrigo *et al.*, 2001). While the temperature signal embedded within eastern hemlock ring widths tends to be limited to a short period of the growing season—mainly early spring, March—the strongest seasonal temperature response of LWB extended during the entire growing season, spanning from March until October. Red spruce is a long-lived (>300 years), shade-tolerant conifer with a core distribution in the northeastern US and Canada, and small, disjunct populations extending south to the highest-elevations of the southern Appalachian Mountains on the North Carolina-Tennessee border. The spruce zone, where the species attains its maximum importance in the community, varies across the geographic range (Adams *et al.*, 2012). In the northern part of its range, the spruce zone occurs at low to high elevations (<650->950 m asl) (Foster and D'Amato, 2015; Kosiba *et al.*, 2018). At southern range margins, the spruce zone is only found at high elevation (>1,400 m asl) (McLaughlin *et al.*, 1987). Like AWC and eastern hemlock, red spruce has also been shown to exhibit relationships between ring width and temperature (Cook, 1987; Johnson *et al.*, 1988; Cook and Johnson, 1989; Federer *et al.*, 1989).

During the period 1900–2012, monthly correlations were consistently higher for LWB compared to RW during every month tested (Figure S1), as well as for Mar-Oct T_{mean} at each site (Figure 2). Correlations between Mar-Oct T_{mean} and RW were all $r < .30$, $p = .10$. Each LWB site expressed robust, positive correlations with Mar-Oct T_{mean}, with 5 of 6 sites returning correlations that were above 0.50 ($r > .50$, $p < .0001$). The weakest site was Bradbury, though still significant ($r = .46$, $p < .0001$). BI is a representation of wood density that, in turn, is defined by tracheid dimensions and cell wall density (Campbell *et al.*, 2007; McCarroll *et al.*, 2002; Rydval *et al.*, 2014. Latewood density is mainly driven by cell

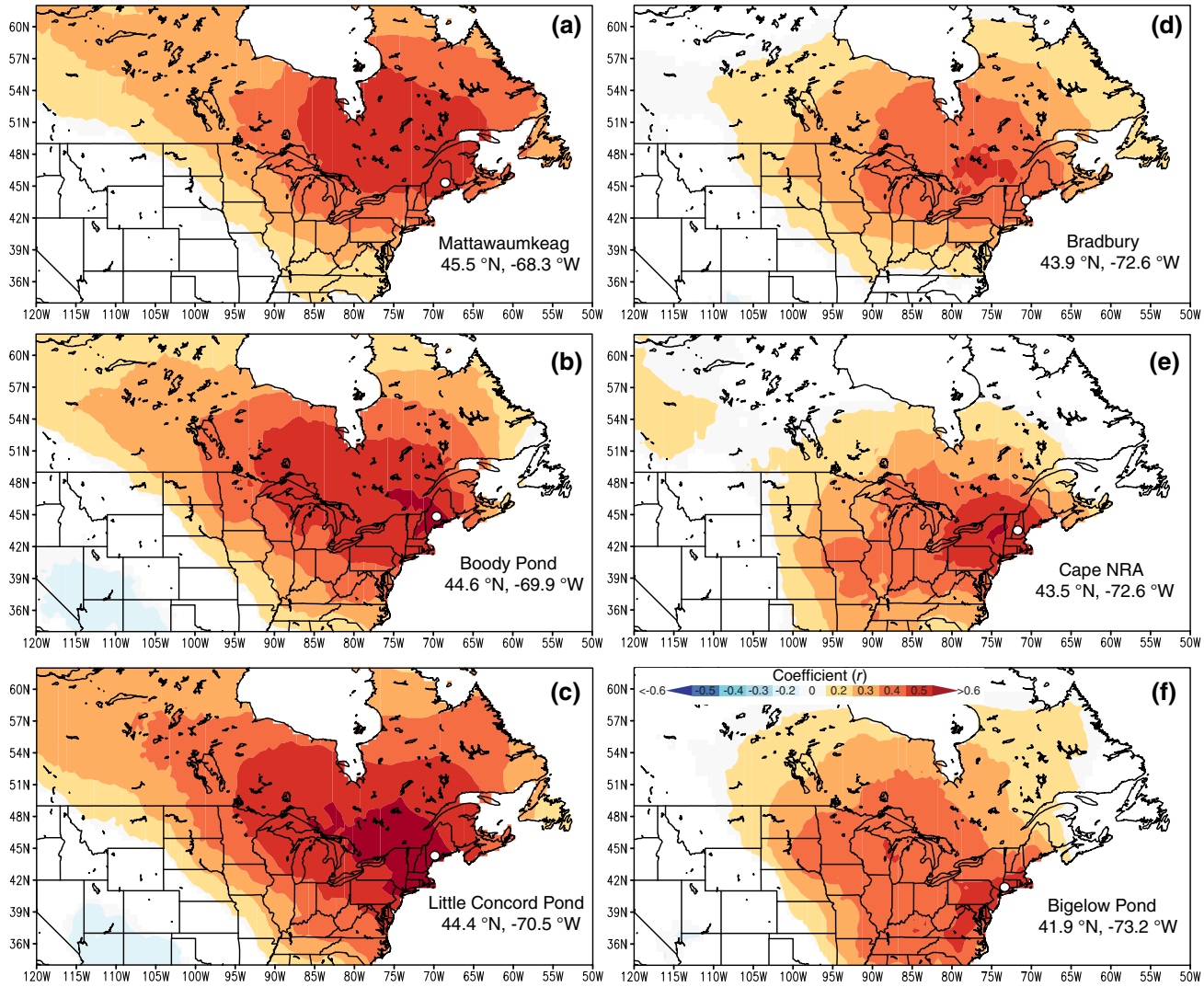

FIGURE 3 Northeast (NE) individual site spatial correlations with temperature. Maps show location of each NE site (white circle) spatial correlations (first differenced) with the gridded CRU TS mean March–October temperature field during the period 1900–2012

wall area—higher temperatures allow more cell wall material to be incorporated in each latewood cell. Thus, temperature appears to be the main limiting factor for the density of the latewood in red spruce and eastern hemlock, while moisture availability is likely the primary limiting factor of ring widths, as recently concluded by Maxwell *et al*. (2020) for these sites. Dependent upon site conditions, relationships between eastern hemlock ring widths with both moisture availability and temperature is well-established (e.g., Lutz, 1944; Cook and Cole, 1991; D'Arrigo *et al*., 2001; Saladyga and Maxwell, 2015). LWB chronologies from both hemlock and red spruce from the Northeast sites demonstrated a broad regional expression with Mar-Oct T_{mean} (Figure 3). Little Concord Pond showed the strongest regional signal, with correlations exceeding 0.60 interpolated over the CRU gridded field from northern New Jersey to central Maine and across southern Quebec and Ontario (Figure 3c). This spatial signature was common across all other chronologies as well (Figure 3a–f), just slightly weaker for Bradbury (Figure 3d).

Despite showing strong chronology agreement across sites, we could not find a discernible temperature signal within any of the LWB chronologies across the Midwest (Figure 2). This was a confounding result, especially given the high level of crossdating noted between measured samples, as well as RBAR of the individual detrended site chronologies. We did, however, detect negative correlations between RW at Pine Hills and Liar's Bench and Jun-Aug T_{max}, as well as positive correlations with Jun-Aug drought (drought results not shown, but discussed below).

Across the Southeast sites, we identified strong and positive relationships between individual DBI site

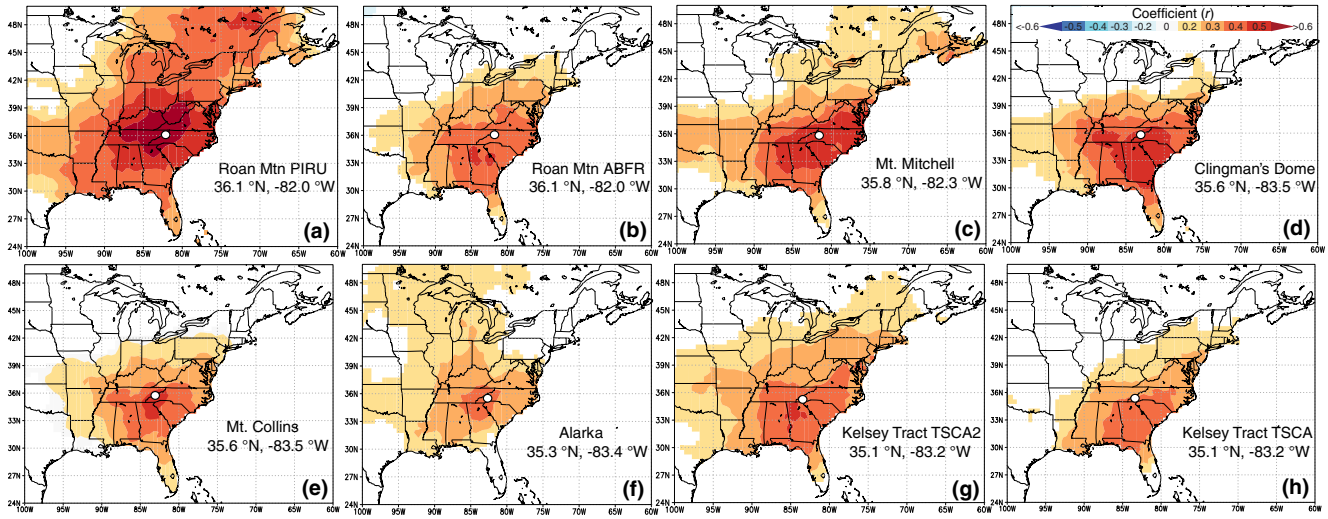

FIGURE 4 Southeast (SE) individual site spatial correlations with temperature. Maps show location of each SE site (white circle) spatial correlations (first differenced) with the gridded CRU TS mean September–October temperature field during the period 1950–2008/2018, depending on length of chronology detailed in Table 1. PIRU = *Picea rubens*; ABFR = *Abies fraseri*; TSCA = *Tsuga canadensis*; TSCA2 = *Tsgua caroliniana*

chronologies and maximum late summer/early fall temperatures (T_{max}) during the September–October months ($r > .40$, $p < .0001$). Correlations between each DBI chronology and T_{mean} also showed strong and significant results, though slightly weaker (not shown); thus we proceeded with T_{max} for the Southeast. This finding was also presented and discussed by Heeter *et al*. (2019). As with the Northeast, we tested monthly (Jan-Dec) correlations for each site, and temperatures averaged over the Sep-Oct time period were consistent in producing the strongest temporal and spatial relationships (Figure S2). Correlations were consistently higher for DBI compared to RW during the target season, late summer/early fall (Figure 2; Figure S1). We also tested T_{mean} against each DBI site chronology, with both temporal and spatial correlation tests producing much weaker results compared to T_{max}. Thus, T_{max} results during the Sep-Oct period are shown. We also noted a marked decoupling between instrumental T_{max} and each DBI chronology prior to the ca. 1945–1950 period for both the CRU and PRISM data sets. This was also found and discussed by Heeter *et al*. (2019) for an earlier version (e.g., fewer samples) of the Roan Mtn red spruce record. They attributed this drop in signal to low sample depth and a sharp decrease in EPS. However, in this study we added more red spruce samples to the Roan Mtn red spruce chronology, such that the record now carries a strong common signal back to 1912. Hence, we do not expect the decoupling between T_{max} and DBI at the ca. 1945–1950 period to be caused by a drop in signal in the new, updated record. This prompted us to investigate the temporal aspects of the instrumental CRU TS4.03 temperature data sets. We found a total of 281 input stations within the Southeast region (37–33°N, 84–81°W; requiring at least 10 years of data). However, many of these stations were installed post World War II and start recording during the ca. 1945–1950 period. Additionally, very few stations up until the 1950s are representative of upper elevations (> ca. 500 m). Thus, we restrict analysis for the Southeast sites to begin in the year 1950.

As shown for the Northeast, DBI-temperature correlations outperformed RW. Yet in the Southeast, we noted varied climate responses of RW across species. All red spruce RW records demonstrated weak, yet significant ($\alpha = 0.90$), relationships with Sep-Oct mean T_{max}. Like eastern hemlock, red spruce is a shade-tolerant, evergreen conifer native to the East that prefers cool, moist habitats. Red spruce ring-width chronologies from numerous sites across the Southern Appalachians were negatively correlated with previous summer (Aug) temperatures and positively correlated with early winter (Dec) temperatures (Cook, 1987; Johnson *et al*., 1988; Cook and Johnson, 1989; Federer *et al*., 1989). Two RW records, however, showed no detectable temperature signal (Roan Mt. Fraser fir and Kelsey Tract eastern hemlock), while the Carolina hemlock RW record from Kelsey tract showed a moderate, negative response to late summer T_{max} ($r = .34$, $p < .10$). In a similar finding, Austin *et al*. (2016) reported a Carolina hemlock chronology from Bluff Mountain, North Carolina to be significantly and positively correlated to summer drought (May-Oct) and negatively correlated to summer temperatures ($r > .30 < .40$, $p = .05$). Bluff Mountain is located in northwest North Carolina/northeast Tennessee region,

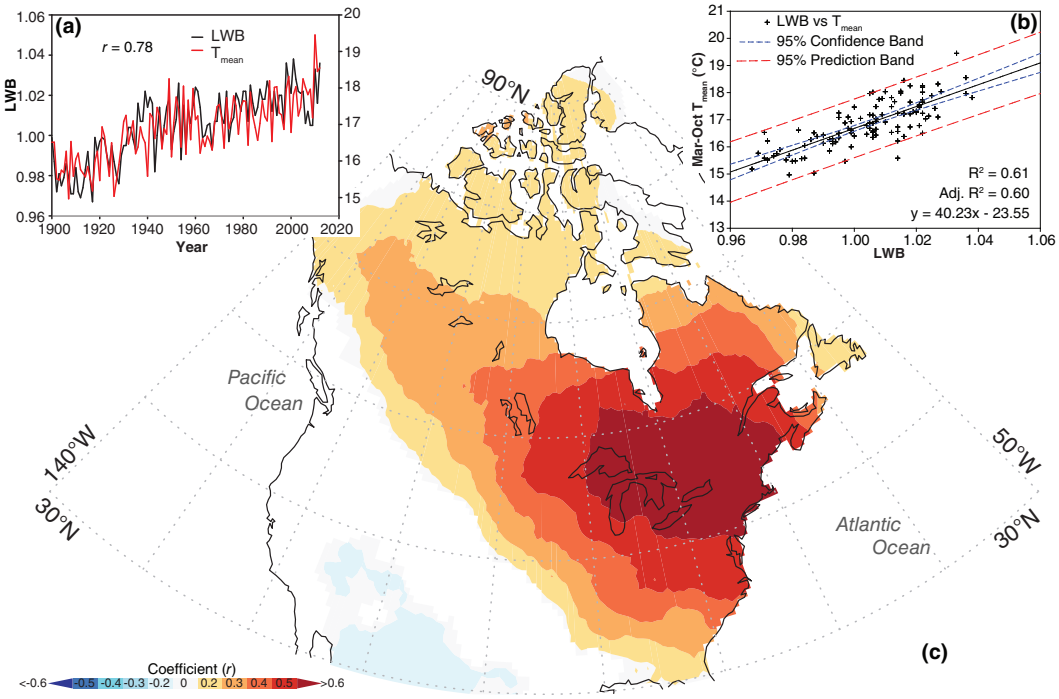

FIGURE 5 Regional expression of the Northeast LWB chronologies. (a) Relationship between the composite (all 6 sites) LWB chronology and T_{mean} over the region ($r = .78$; nontransformed). (b) Linear regression model between Mar-Oct instrumental T_{mean} and the 6-site composite LWB chronology ($R^2 = 0.61$; nontransformed). (c) Spatial correlations (first differenced) between PC_1 for the 6-site LWB group from the NE region and Mar-Oct T_{mean} CRU TS temperature

ca. 206 km north of the Kelsey Tract site in southwestern North Carolina.

The 8 DBI records from the Southeast showed a similar spatial correlation pattern when compared to gridded Sep-Oct T_{max}, despite slight strength variations (Figure 4a–h). The red spruce DBI record from Roan Mtn showed the strongest and broadest regional expression, with the highest correlation interpolation polygon ($r > .60$) covering West Virginia to the north and extending across Kentucky, North Carolina, Tennessee, and northern Georgia (Figure 4a). The additional samples added to the previous DBI chronology reported by Heeter *et al.* (2019) improved the RBAR, EPS, and temporal and spatial correlations of the updated Roan Mtn red spruce chronology. A similar pattern to Roan Mtn red spruce is also seen with Mt. Mitchell, Clingman's Dome, and Mt. Collins. As the site located at the lowest elevation, Alarka showed the weakest regional spatial signal, although still statistically significant ($p < .10$). Because the temperature signal was more robust in all BI chronologies compared to RW, we proceed with further analyses using BI only.

3.3 | BI signal homogeneity

A correlation matrix between the Northeast site LWB chronologies showed a high level of agreement among sites. Relationships between each chronology were statistically significant, save for two: Mattawaumkeag-Bigelow Pond and Cape NRA-Bigelow Pond ($p > .10$). Most intersite correlations in the matrix ranged .30–.60, with the highest between Boody Pond and Little Concord Pond ($r = .67$). Individual site LWB records also showed similar trends during the common period of overlap (1926–2009), marked by an increase in LWB after ca. 1960 (Figure S3).

For all LWB chronologies, the explained variance on the first eigenvector (PC_1) was 45.6%. We noted a relationship between the latitude location of a site and stronger loading on PC_1 ($R^2 = 0.63$; Figure S4). This agrees with results presented by Cook and Cole (1991). After mapping temperature correlations from 42 eastern hemlock sites distributed across the species range in the East, they found a general increase in March temperature correlations towards the western (e.g., Upper Peninsula Michigan and Great Lakes region) and northern (e.g., north-central Maine) range limits. The weakest site to load on PC_1 was also the lowest latitude site, Bigelow Pond, Connecticut. Whereas, the second-highest latitude site, Boody Pond, Maine, represented the strongest loading of the Northeast sites to PC_1. The highest-latitude site, Mattawaumkeag, was the third strongest loading. However, we do note that Mattawaumkeag was located

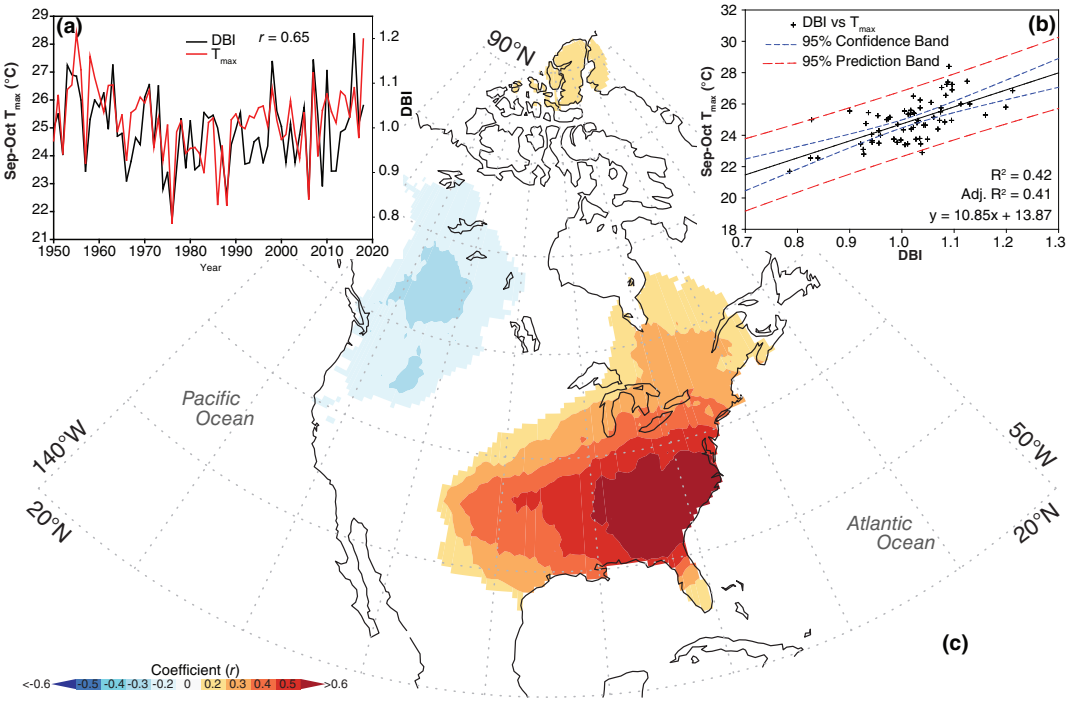

FIGURE 6 Regional expression of the Southeast DBI chronologies. (a) Relationship between the composite (all 8 sites) DBI chronology and T_{max} over the region ($r = .65$; nontransformed). (b) Linear regression model between Sep-Oct instrumental T_{max} and the 8-site composite DBI chronology ($R^2 = 0.42$; nontransformed). (c) Spatial correlations (first differenced) between PC_1 for the 8-site DBI group from the SE region and Sep-Oct T_{max} CRU TS temperature

at the lowest elevation, although there was no relationship between PC_1 loading and elevation ($R^2 = 0.008$, $p > .10$). This was expected because eastern hemlock is a mesic, cove species and is not known for inhabiting upper elevation sites, unlike red spruce. We do note, however, that these correlations were made with few data points, and interpretation should be done with caution. We expect the relationship between elevation and PC_1 loading to change and become more clear as more high elevation, red spruce sites across Maine, New Hampshire,

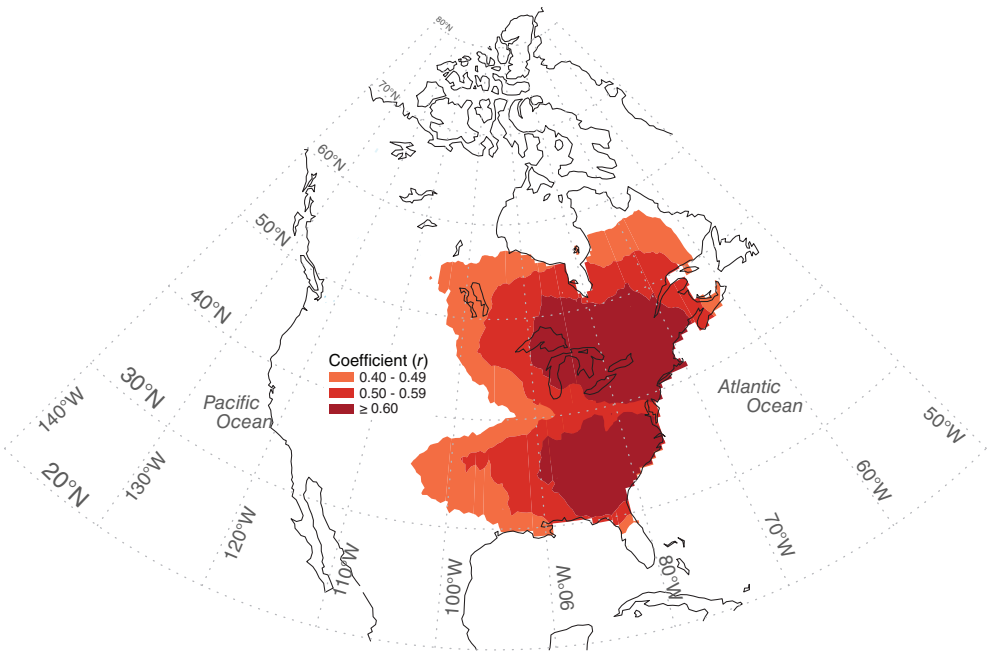

FIGURE 7 Spatial expression of the current Eastern North American temperature network. Plotted over space are the $r > .40$, .50, and .60 correlation (first differenced) polygons from the Northeast and Southeast regions for respective temperature parameters, seasons, and periods of time

Vermont, and New York are added to the Northeast network.

Although each LWB chronology in the Midwest showed strong agreement among measured series at the site level, the correlation matrix showed no agreement, and even anti-correlation, between sites during the common period of overlap (1959–2013). Cliff Forge showed no relationship between Liar's Bench or Pine Hills. Though, we did find that Liar's Bench and Pine Hills were strongly anti-correlated (Figure S5). Because Midwest sites (a) failed to demonstrate individual site relationships between LWB and temperature, and (b) showed poor inter-site chronology relationships, we did not perform a PCA between Midwest sites and do not include the Midwest sites in further analyses. Although the Midwest sites failed to demonstrate a valuable climate signal for reconstruction purposes, these results suggest that latitude and elevation play an important role in the controlling factor of temperature on latewood density in conifers, and hence the utility of BI for temperature analyses. The lack of a LWB temperature signal from the Midwest sites could be due to (a) specific ecological site characteristics unlike the eastern hemlock from the Northeast region, or (b) differences in climate regime between the Midwest region and Northeast and Southeast. We do note that, while most of the conterminous US has experienced some level of warming since ca. 1900, large parts of the Midwest, including Indiana and Ohio, have experienced cooling summer temperature extremes (e.g., Hansen *et al*., 2001), possibly due to the increase in agricultural practices which can alter surface energy budgets (Mueller *et al*., 2016; Nikiel and Eltahir, 2019). Thus, trees in this portion of the Midwest have likely not experienced the same level of temperature stress as communities we sampled in the highest elevations of the Appalachian Mountains or in the Northeast. Based on the principle of limiting factors, trees are unlikely to produce a clear temperature signal if not stressed at some level by temperature variability (Fritts, 1976). Wilson *et al*. (2019) reported a similar finding for one of their 17 white spruce sites from the Yukon. The utility of BI for temperature response might be influenced by trees growing at ecologically distinct sites, potentially influenced by geomorphic activity, or located at drier, lower elevation sites. Further explorations with eastern hemlock and other viable species in the Midwest from higher latitudes will be critical to a westward expansion of the network in the East. For example, Michigan (lower and upper) hosts many long-lived, potentially temperature-sensitive eastern hemlock and eastern white pine (*Pinus strobus* L.) collections available on the ITRDB.

Despite the inclusion of 4 different species in the Southeast region, the 8 DBI records showed a high level of inter-site agreement (Figure S6). The strongest agreement was between the two co-occurring hemlock chronologies at the Kelsey Tract site, though not surprising given they derive from the same genus. At the Roan Mtn site, the red spruce and Fraser fir DBI chronologies showed significant agreement, yet weaker compared to Kelsey Tract. Although co-occurring on Roan Mtn, the weak association could be a result of varying genus characteristics. Another particularly strong association was between Alarka and Mt. Mitchell. Both DBI chronologies share the same RBAR (0.27) and signal strength characteristics, despite being from different elevations and latitudes. The only insignificant relationships were between the Kelsey Tract Carolina hemlock and both Clingman's Dome and Roan Mtn red spruce.

After running a PCA among the Southeast sites, the explained variance of PC_1 was 40.8%. The strongest loading to PC_1 was Roan Mtn red spruce and the weakest was Mt Mitchell. The nonlinear relationship between latitude and PC_1 loading ($R^2 = 0.11$) is visualized in Figure S4. Further, we did not find a relationship between elevation and PC_1 loading ($R^2 = 0.007$), though, like the Northeast, most sites were clustered within a small elevation range of ca. 100 m. To determine the influence of including multiple species, we also plotted only the red spruce sites from the Southeast, this time against the correlation coefficient of each chronology with Sep-Oct T_{max} over the region. We noticed significant relationships between T_{max} and both latitude ($R^2 = 0.84$) and elevation ($R^2 = 0.65$).

3.4 | Regional expression

To highlight the strength of BI metrics across the Northeast and Southeast regions, we compared both the composite LWB/DBI chronology from all sites in respective regions and PC_1 against a gridded temperature field. Across the Northeast, we found strong and positive association between LWB (nontransformed) and Mar-Oct T_{mean} during the period 1900–2012 ($r = .78$, $p < .0001$). Not only is LWB a robust predictor of growing season temperature trends since 1900, but the instrumental record and LWB time series have similar variance, with no major model under- or over-predictions ($R^2 = 0.61$, Adj. $R^2 = 0.60$, $p < .0001$; Figure 5a,b). When comparing the first differenced versions of LWB PC_1 and gridded CRU temperatures, the relationship explains >60% of the variance across a large region concentrated in the Northeast US and eastern Canada and across to the Great Lakes region to the west. Strong relationships are also seen ($r > .50$) to the south down to North Carolina, west through the Midwest, and north covering most of Ontario and the southern portion of Quebec.

We found a similar pattern for the composite DBI chronology combined from all 8 sites across the Southeast region. DBI is a strong predictor of regional Sep-Oct T_{max}, and despite short periods of under-prediction during the 1990s and 2010–2011, instrumental temperature and DBI shared similar variance (Figure 6a). Although weaker than the Northeast composite LWB chronology, a model between DBI and Sep-Oct T_{max} explained 42% of the instrumental variance during the period 1950–2018 (Figure 6b). The spatial pattern of PC_1 versus gridded T_{max} showed a strong concentration across the Southeast US region, even showing significant explanations of temperature down the Florida peninsula (r = .20–.59). The $r > .50$ polygon extends from northern Florida west throughout the lower Mississippi River Valley and north to the Mid-Atlantic region (e.g., Virginia, Maryland, Delaware).

3.5 | Eastern North America temperature network

The development of a network of BI-derived temperature proxies across Eastern North America is not only possible, but critical to better understanding past temperature variability across this broad region. Just with the 14 sites included in this study (6 from Northeast, 8 from Southeast), there is considerable overlap between the $r > .40$ and .50 polygons across eastern North America (Figure 7). The highest correlation polygons ($r > .60$) for the Northeast and Southeast almost overlap, save for a small sector of the US Mid-Atlantic region. However, targeting red spruce and eastern hemlock sites in this region, such as in higher elevations of West Virginia, Virginia, and Pennsylvania will be critical to expanding the spatial prediction power of the network. Given the East is a heavily disturbed biome, the potential influence of various disturbances on BI metrics will need to be considered.

3.5.1 | Disturbance

Plant communities across the East, particularly those that include red spruce and eastern hemlock, have been repeatedly altered by biological (e.g., hemlock woolly adelgid (HWA; *Adelges tsugae* Annand; Orwig and Foster, 1998; Saladyga and Maxwell, 2015), eastern spruce budworm (*Choristoneura fuminferana* Clem.; Fraver *et al.*, 2007), balsam woolly adelgid; Dale *et al.*, 1991), chemical (e.g., acid deposition; Johnson and Siccama, 1983; Johnson, 1983; McLaughlin *et al.*, 1993), and physical (e.g., winter foliar injury; Kosiba *et al.*, 2013; Wason and Dovciak, 2017), logging; White *et al.*, 2012; White *et al.*, 2014) disturbances, especially in recent decades. As this project continues and red spruce and eastern hemlock are targeted across the East for expansion of the network, attention needs to be allocated towards ensuring that BI data are not influenced by various disturbances. As such, we tested the temporal stability in relationships between the NE and SE BI metrics and instrumental temperature. We noted stationary relationships between BI metrics from the NE and SE sites and instrumental temperatures over time (Figure S7). Although the regression slope for the NE sites increases slightly over the 1900–2012 period, we observed a consistent positive effect of Mar-Oct T_{mean} on LWB. Even stronger, however, was the stability of the SE-T_{max} (Sep-Oct) relationship during the period 1950–2008, noted as a consistent and positive effect on DBI. Thus, the climate signal within the DBI measured across the SE sites does not appear to be adversely contaminated by the effects of ecological disturbances. In 2003, a severe winter injury event caused foliar damage in ca. 90% of red spruce across the northeastern US (Kosiba *et al.*, 2013). Whereas this event led to a 3-year decline in RW at sites tested in Vermont, New Hampshire and Massachusetts, we did not notice any influence in the Cape NRA red spruce LWB data around this time, either graphically or statistically. For the remainder of the NE sites, all of which are eastern hemlock, they were sampled before the spread of HWA into the region. Across the NE sites, we noted strong and temporally stable relationships between LWB and temperature, at least until 2012. As LWB chronologies are updated to the present, the potential influence of acidic deposition, HWA, and other disturbances will need to be tested.

HWA is a non-native, invasive pest that attacks and kills eastern and Carolina hemlock trees. HWA was introduced to the East from Asia in the 1950s, and has spread rapidly across the northeast and mid-Atlantic regions, especially into the Southern Appalachians (Lovett *et al.*, 2006; Nuckolls *et al.*, 2009; Roberts *et al.*, 2009; Elliott and Vose, 2011). As of 2010, HWA was documented in the counties of southern North Carolina, including that of the Kelsey Tract (Vose *et al.*, 2013). HWA has been shown to decouple the relationship between RW and climate in the Southeast US (Saladyga and Maxwell, 2015). We did not notice a regime shift in DBI time series from the two Kelsey Tract hemlock species, as has been shown for eastern hemlock RW (Saladyga and Maxwell, 2015). We do note, however, an anomalously low DBI values during the 2009–2010 period, but this is most likely due to anomalously low temperatures during that period (Eck *et al.*, 2019), followed by a recovery post-2010. Across the SE sites, we

noted strong and temporally stable relationships between DBI and temperature.

3.5.2 | Viable species

We found red spruce to have the greatest potential for reconstructing temperature using BI in the Southeast region, and both red spruce and eastern hemlock for the Northeast. In the late 1970s/early 1980s, Dr. Laura Conkey led pioneering research focused on measuring MXD in red spruce from the Northeast for the purposes of reconstructing temperature (Conkey, 1979; Conkey, 1984; Conkey, 1986). Conkey was the first to test the efficacy of using MXD for temperature response in eastern North America (Conkey, 1986). After measuring MXD across 3 red spruce sites in Maine, she found MXD-Apr-May R^2 models ranged from 33 to 37% variance explained. Conkey (1986) identified red spruce growing at high elevations in New England as an ideal candidate for reconstructing temperature using wood density. Sheppard *et al*. (1996) successfully developed a model of mean early growing season temperatures back to the early 19th century using experimental brightness analysis of latewood in red spruce. However, these two previous studies were spatially and temporally limited. Other correlation analyses of the influence of temperature on annual radial growth of red spruce from New England sites (Conkey, 1979; Conkey, 1984; Cook and Johnson, 1989; Kosiba *et al*., 2018) have identified positive annual relationships with monthly mean temperatures during the preceding fall and winter and the current spring, and with both low temperatures and above-normal precipitation in July and August of the preceding summer. Currently, there are only a few reported tree-ring proxies of temperature in the New England region of the eastern US (e.g., Conkey, 1986; Cook and Johnson, 1989; Pearl *et al*., 2017; Pearl *et al*., 2020). These reconstructions use RW and wood density parameters as paleoclimate proxies and are limited to the far north/northeastern margins of maritime Maine and do not capture more continental climate effects of the region.

In an important step towards developing a broad-scale spatial field reconstruction of temperature for the East, Pearl *et al*. (2020) developed a skilful gridded reconstruction of Jan-Aug T_{mean} that explained up to 47% of instrumental variance for some grid points. Spatially, grid point models located in coastal areas of New Jersey, New York, Connecticut, and Massachusetts displayed high predictive skill and were well-validated. However, grid point models located west of 78°W, north of 47.5°N, and south of 39°N failed to pass cross-calibration and verification statistics. Adding BI or RW measured from the Pearl *et al*. (2017) and Pearl *et al*. (2020) collections could serve to produce a skilful spatial temperature field reconstruction that covers a broader scale in the East. However, considering other species for BI utility is critical in developing the broad-scale temperature network across the East.

Alexander *et al*. (2019) used a multi-species network of tree-ring chronologies ($n = 228$ from 29 different species; 90% total ring width, 4% earlywood width, 3% latewood width, 3% MXD) across the Northeast US network to test the hypothesis that an increase in species diversity among the pool of predictors improves reconstructions of past temperatures. They found AWC alone explained 31% ($r = .56$) of instrumental winter temperatures, but expanding that model to include multiple species improved the explained variance to 44% ($r = .67$) during the period 1900–1970. The species that were the strongest predictors of Jan-Apr minimum temperatures were AWC, eastern hemlock, tulip tree (*Liriodendron tulipifera* L.), red spruce, and eastern white pine, each explaining ca. 10–20% of explained variance in the model. Alexander *et al*. (2019) study shows that taking a multi-proxy approach to reconstructing temperatures across the East could improve the explanatory power of a model above just using one proxy, especially given the strong temporal and broad spatial signature of BI across the East (Figure 7).

3.5.3 | Conclusions

We demonstrate the strong potential of developing a broad-scale, long-term gridded temperature field reconstruction for eastern North America. However, certain key elements will need either to be addressed or improved before such a task is accomplished. First, new site collections need to be targeted in the Mid-Atlantic to increase the explanatory power across that region and provide a link between the Southeast and Northeast regions. Several red spruce and/or hemlock sites exist on the ITRDB from West Virginia, Virginia, Pennsylvania, and New York, as these will be sites critical to this effort. In addition, collections in new areas, such as the Great Lakes region of the US and Canada, need to be targeted for inclusion. A number of eastern hemlock collections exist on the ITRDB from this region, some of which extend into the 15th century, but are in dire need of updating (Hessl and Pederson, 2013). Also noteworthy from this region are long-lived eastern white pine, as well as the millennial-length potential of a northern white-cedar (*Thuja occidentalis* L.) record from the Niagara Escarpment (Larson and Kelly, 1991; Kelly and Larson, 1997). BI measured in Alaskan yellow-cedar

(*Callitropsis nootkatensis* [D. Don] Oerst. ex D.P. Little) was shown recently to contain a robust temperature signal from sites in Alaska (Wiles *et al*., 2019). Although the two derive from different genera, they belong to the same Cupressaceae family and have similar wood characteristics. Second, the difference in metric (T_{max} versus T_{mean}) and season (Sep-Oct versus Mar-Oct) between the Southeast and Northeast regions, respectively, will need to be addressed. Though, calibration with high-pass filtered tree-ring data as well as climate data should help to clean this up. While the exact months of temperature reconstruction might not be exactly the same between regions, a consistent target season should be possible (e.g., summer or late-summer). Further, because both T_{mean} and T_{max} showed similar results for the Southeast—particularly demonstrated by Heeter *et al*. (2019)—and Northeast sites, a consistent temperature metric should also be possible. Third, because our NE BI chronologies end in 2012, updates will need to be performed at these and additional sites so the regional record is extended to the end of the current decade. Given that HWA has only spread to the southern portions of Vermont, New Hampshire, and Maine, finding living eastern hemlock individuals should be possible. Third, BI chronologies across the entire network, both in the Southeast and Northeast and across the Great Lakes region will need to be extended as far back in time as possible. By soliciting collaborators with private collections, taking advantage of the numerous collection from the ITRDB, or exploring remnant material from historical structures or lacustrine environments, this could be accomplished. However, obtaining the actual tree-ring samples from archives is needed in order to measure BI, and there will likely be logistical challenges of finding and incorporating remnant material from viable species (e.g., use of eastern hemlock or red spruce in historical structures was rare). Hence, developing the Eastern North American Temperature Network for the purposes of producing a spatial temperature field reconstruction will be a highly collaborative venture.

ACKNOWLEDGEMENTS

This research is funded by the US National Science Foundation Paleo Perspectives on Climate Change program (P2C2; AGS-1805276 and AGS-2002524) and the Geographical Sciences Program (BCS-1229887). We wish to thank the following: Dr. Saskia van de Gevel and Phil White for donation of the Roan Mtn red spruce and Fraser fir collections; Tsun Fung Au, Benjamin Lockwood, Laura Smith, Joshua Bregy, and Danny King for field assistance in the Smokey Mountains; Gary Wein at the Highlands-Cashiers Land Trust for assistance in the field at Kelsey Tract. We appreciate access to sites provided by Great Mountain Forest, Howland, Maine Division of Parks and Public Lands, Mattawamkeag Wilderness Park, New Hampshire Division of Forests and Lands, The Nature Conservancy, University of Maine, and the US Forest Service and Stacy Nowacki for field assistance. We also thank Charles V. Cogbill, Alexandra Kosiba, Kathryn Daly and Matthew Tierney for field assistance at the Cape NRA and permission to sample from Jennifer Pontius at the USFS Northern Research Station. We thank two anonymous reviewers for helpful comments and suggestions that improved earlier drafts of this manuscript.

ORCID

Grant L. Harley https://orcid.org/0000-0003-1557-8465

REFERENCES

Adams, M.B., Cogbill, C., Cook, E., DeHayes, D., Fernandez, I., Jensen, K., Johnson, A., Johnson, D., Kohut, R., McLaughlin, S., et al. (2012) *Ecology and Decline of Red Spruce in the Eastern United States*, Vol. 96. New York, NY: Springer Science & Business Media.

Alexander, M.R., Pearl, J.K., Bishop, D.A., Cook, E.R., Anchukaitis, K.J. and Pederson, N. (2019) The potential to strengthen temperature reconstructions in ecoregions with limited tree line using a multispecies approach. *Quaternary Research*, 92, 583–597.

Anchukaitis, K.J., D'Arrigo, R.D., Andreu-Hayles, L., Frank, D., Verstege, A., Curtis, A., Buckley, B.M., Jacoby, G.C. and Cook, E.R. (2013) Tree-ring-reconstructed summer temperatures from Northwestern North America during the last nine centuries. *Journal of Climate*, 26, 3001–3012.

Austin, D.A., van de Gevel, S.L. and Soulé, P.T. (2016) Forest dynamics and climate sensitivity of an endangered carolina hemlock community in the southern appalachian mountains, USA. *Botany*, 94, 301–309.

Bishop, D.A., Beier, C.M., Pederson, N., Lawrence, G.B., Stella, J.C. and Sullivan, T.J. (2015) Regional growth decline of sugar maple (*Acer saccharum*) and its potential causes. *Ecosphere*, 6, 1–14.

Björklund, J., Gunnarson, B.E., Seftigen, K., Esper, J. and Linderholm, H. (2014) Blue intensity and density from northern fennoscandian tree rings, exploring the potential to improve summer temperature reconstructions with earlywood information. *Climate of the Past*, 10, 877–885.

Björklund, J., von Arx, G., Nievergelt, D., Wilson, R., Van den Bulcke, J., Günther, B., Loader, N., Rydval, M., Fonti, P., Scharnweber, T., et al. (2019) Scientific merits and analytical challenges of tree-ring densitometry. *Reviews of Geophysics*, 57, 1224–1264.

Briffa, K.R., Jones, P. and Schweingruber, F. (1992) Tree-ring density reconstructions of summer temperature patterns across western North America since 1600. *Journal of Climate*, 5, 735–754.

Briffa, K.R., Jones, P.D. and Schweingruber, F.H. (1988) Summer temperature patterns over Europe: a reconstruction from 1750 ad based on maximum latewood density indices of conifers. *Quaternary Research*, 30, 36–52.

Briffa, K.R., Osborn, T.J., Schweingruber, F.H., Harris, I.C., Jones, P.D., Shiyatov, S.G. and Vaganov, E.A. (2001) Low-frequency temperature variations from a northern tree ring density network. *Journal of Geophysical Research: Atmospheres*, 106, 2929–2941.

Burns, R. M., Honkala, B. H. et al. (1990) Silvics of North America. Volume 1. Conifers. *Agriculture Handbook (Washington)*.

Campbell, R., McCarroll, D., Loader, N.J., Grudd, H., Robertson, I. and Jalkanen, R. (2007) Blue intensity in *Pinus sylvestris* tree-rings: developing a new palaeoclimate proxy. *The Holocene*, 17, 821–828.

Conkey, L. (1984) *Dendrochronology and Forest Productivity: Red Spruce Wood Density and Ring Width in Maine*. Bangor, ME: USDA Forest Service general technical report NE-United States, Northeastern Forest Experiment Station.

Conkey, L.E. (1979) Response of tree-ring density to climate in Maine, USA. *Tree-Ring Bulletin*, 39, 29–38.

Conkey, L.E. (1986) Red spruce tree-ring widths and densities in eastern North America as indicators of past climate. *Quaternary Research*, 26, 232–243.

Cook, E.R. (1987) The decomposition of tree-ring series for environmental studies. *Tree-Ring Bulletin*, 47, 37–59.

Cook, E.R. and Cole, J. (1991) On predicting the response of forests in Eastern North America to future climatic change, 19, 271–282.

Cook, E.R. and Johnson, A.H. (1989) Climate change and forest decline – a review of the red spruce case. *Water Air and Soil Pollution*, 48, 127–140.

Dale, V., Gardner, R., DeAngelis, D., Eagar, C. and Webb, J. (1991) Elevation-mediated effects of balsam woolly adelgid on southern Appalachian spruce–fir forests. *Canadian Journal of Forest Research*, 21, 1639–1648.

Daly, C., Halbleib, M., Smith, J.I., Gibson, W.P., Doggett, M.K., Taylor, G.H., Curtis, J. and Pasteris, P.P. (2008) Physiographically sensitive mapping of climatological temperature and precipitation across the conterminous United States. *International Journal of Climatology: A Journal of the Royal Meteorological Society*, 28, 2031–2064.

D'Arrigo, R.D., Schuster, W.S., Lawrence, D.M., Cook, E.R., Wiljanen, M. and Thetford, R.D. (2001) Climate-growth relationships of eastern hemlock and chestnut oak from black rock forest in the highlands of southeastern New York. *Tree-Ring Research*, 57, 183–190.

Dolgova, E. (2016) June–september temperature reconstruction in the northern caucasus based on blue intensity data. *Dendrochronologia*, 39, 17–23.

Durbin, J. and Koopman, S.J. (2012) *Time Series Analysis by State Space Methods*. New York, NY: Oxford University Press.

Eck, M.A., Perry, L.B., Soulé, P.T., Sugg, J.W. and Miller, D.K. (2019) Winter climate variability in the southern appalachian mountains, 1910–2017. *International Journal of Climatology*, 39, 206–217.

Elliott, K.J. and Vose, J.M. (2011) The contribution of the coweeta hydrologic laboratory to developing an understanding of long-term (1934–2008) changes in managed and unmanaged forests. *Forest Ecology and Management*, 261, 900–910.

Esper, J., Cook, E.R. and Schweingruber, F.H. (2002) Low-frequency signals in long tree-ring chronologies for reconstructing past temperature variability. *Science*, 295, 2250–2253.

Federer, C., Tritton, L., Hornbeck, J. and Smith, R. (1989) Physiologically based dendroclimate models for effects of weather on red spruce basal-area growth. *Agricultural and Forest Meteorology*, 46, 159–172.

Foster, J.R. and D'Amato, A.W. (2015) Montane forest ecotones moved downslope in northeastern USA in spite of warming between 1984 and 2011. *Global Change Biology*, 21, 4497–4507.

Frank, D., Büntgen, U., Böhm, R., Maugeri, M. and Esper, J. (2007) Warmer early instrumental measurements versus colder reconstructed temperatures: shooting at a moving target, 26, 3298–3310.

Fraver, S., Seymour, R.S., Speer, J.H. and White, A.S. (2007) Dendrochronological reconstruction of spruce budworm outbreaks in northern Maine, USA. *Canadian Journal of Forest Research*, 37, 523–529.

Fritts, H. (1976) *Tree Rings and Climate*. Tucson, AZ: Elsevier.

Hansen, J., Ruedy, R., Sato, M., Imhoff, M., Lawrence, W., Easterling, D., Peterson, T. and Karl, T. (2001) A closer look at United States and global surface temperature change, 106, 23947–23963.

Harris, I., Jones, P. D., Osborn, T. J. and Lister, D. H. (2013) Updated high-resolution grids of monthly climatic observations: the CRU TS3.10 Dataset.

Heeter, K.J., Harley, G.L., Van De Gevel, S.L. and White, P.B. (2019) Blue intensity as a temperature proxy in the eastern United States: a pilot study from a southern disjunct population of *Picea rubens* (sarg.). *Dendrochronologia*, 55, 105–109.

Hessl, A. and Pederson, N. (2013) Hemlock legacy project (help) a paleoecological requiem for eastern hemlock. *Progress in Physical Geography*, 37, 114–129.

Holmes, R. L. (1983) Computer-assisted quality control in tree-ring dating and measurement.

Hopton, M. and Pederson, N. (2005) Climate sensitivity of Atlantic white cedar at its northern range limit. In: Burke, M.K. and Sheridan, P. (Eds.) *Atlantic White Cedar: Ecology, Restoration and Management: Proceedings of the Arlington Echo Symposium*. Southern Research Station, Asheville, NC: Gen. Tech. Rep. SRS-91., 74. USDA-Forest Service.

Jacoby, G.C. and D'Arrigo, R. (1989) Reconstructed northern hemisphere annual temperature since 1671 based on high-latitude tree-ring data from North America. *Climatic Change*, 14, 39–59.

Johnson, A.H. (1983) Red spruce decline in the Northeastern US: hypotheses regarding the role of acid rain. *Journal of the Air Pollution Control Association*, 33, 1049–1054.

Johnson, A.H., Cook, E.R. and Siccama, T.G. (1988) Climate and red spruce growth and decline in the Northern Appalachians, 85, 5369–5373.

Johnson, A.H. and Siccama, T.G. (1983) Acid deposition and forest decline. *Environmental Science & Technology*, 17, 294A–305A.

Jones, P.D., Briffa, K.R., Barnett, T.P. and Tett, S.F.B. (1998) High-resolution palaeoclimatic records for the last millennium: interpretation, integration and comparison with general circulation model control-run temperatures. *Holocene*, 8, 455–471.

Kalman, R.E. (1960) A new approach to linear filtering and prediction problems. *Transactions of the ASME–Journal of Basic Engineering*, 82, 35–45.

Kelly, P.E. and Larson, D.W. (1997) Dendroecological analysis of the population dynamics of an old-growth forest on cliff-faces of the Niagara escarpment, Canada. *Journal of Ecology*, 85, 467–478.

Kosiba, A.M., Schaberg, P.G., Hawley, G.J. and Hansen, C.F. (2013) Quantifying the legacy of foliar winter injury on woody aboveground carbon sequestration of red spruce trees. *Forest Ecology and Management*, 302, 363–371.

Kosiba, A.M., Schaberg, P.G., Rayback, S.A. and Hawley, G.J. (2018) The surprising recovery of red spruce growth shows links to decreased acid deposition and elevated temperature. *Science of the Total Environment*, 637, 1480–1491.

Larson, D.W. and Kelly, P.E. (1991) The extent of old-growth *Thuja occidentalis* on cliffs of the Niagara escarpment. *Canadian Journal of Botany*, 69, 1628–1636.

Larsson, L. (2014) Coorecorder and cdendro programs of the coorecorder/cdendro package version 7.7.

Lovett, G.M., Canham, C.D., Arthur, M.A., Weathers, K.C. and Fitzhugh, R.D. (2006) Forest ecosystem responses to exotic pests and pathogens in Eastern North America. *Bioscience*, 56, 395–405.

Luckman, B.H., Anchu, K.R., Jones, P. and Schweingruber, F. (1997) Tree-ring based reconstruction of summer temperatures at the Columbia Icefield, Alberta, Canada, ad 1073-1983. *The Holocene*, 7, 375–389.

Lutz, H. (1944) Swamp-grown eastern white pine and hemlock in connecticut as dendrochronological material.

Mann, M.E., Bradley, R.S. and Hughes, M.K. (1999) Northern hemisphere temperatures during the past millennium: inferences, uncertainties, and limitations, 26, 759–762.

Mann, M.E., Zhang, Z., Rutherford, S., Bradley, R.S., Hughes, M.K., Shindell, D., Ammann, C., Faluvegi, G. and Ni, F. (2009) Global signatures and dynamical origins of the little ice age and medieval climate anomaly. *Science*, 326, 1256–1260.

Maxwell, J.T., Harley, G.L., Mandra, T.E., Yi, K., Kannenberg, S.A., Au, T.F., Robeson, S.M., Pederson, N., Sauer, P.E. and Novick, K.A. (2019) Higher CO_2 concentrations and lower acidic deposition have not changed drought response in tree growth but do influence Iwue in hardwood trees in the midwestern United States. *Journal of Geophysical Research: Biogeosciences*, 124, 3798–3813.

Maxwell, R.S., Belmecheri, S., Taylor, A.H., Davis, K.J. and Ocheltree, T.W. (2020) Carbon isotope ratios in tree rings respond differently to climatic variations than tree-ring width in a mesic temperate forest. *Agricultural and Forest Meteorology*, 108014, 288–289.

McCarroll, D., Pettigrew, E., Luckman, A., Guibal, F. and Edouard, J.-L. (2002) Blue reflectance provides a surrogate for latewood density of high-latitude pine tree rings. *Arctic, Antarctic, and Alpine Research*, 34, 450–453.

McLaughlin, S.B., Downing, D.J., Blasing, T.J., Cook, E.R. and Adams, H.S. (1987) An analysis of climate and competition as contributors to decline of red spruce in high elevation Appalachian forests of the eastern United States. *Oecologia*, 72, 487–501.

McLaughlin, S.B., Tjoelker, M.G. and Roy, W. (1993) Acid deposition alters red spruce physiology: laboratory studies support field observations. *Canadian Journal of Forest Research*, 23, 380–386.

Melvin, T. and Briffa, K. (2008) A 'signal-free' approach to dendroclimatic standardisation. *Dendrochronologia*, 26, 71–86.

Mueller, N.D., Butler, E.E., McKinnon, K.A., Rhines, A., Tingley, M., Holbrook, N.M. and Huybers, P. (2016) Cooling of us Midwest summer temperature extremes from cropland intensification. *Nature Climate Change*, 6, 317–322.

Nikiel, C.A. and Eltahir, E.A. (2019) Summer climate change in the midwest and great plains due to agricultural development during the twentieth century. *Journal of Climate*, 32, 5583–5599.

Nuckolls, A.E., Wurzburger, N., Ford, C.R., Hendrick, R.L., Vose, J. M. and Kloeppel, B.D. (2009) Hemlock declines rapidly with hemlock woolly adelgid infestation: impacts on the carbon cycle of southern Appalachian forests. *Ecosystems*, 12, 179–190.

Orwig, D.A. and Foster, D.R. (1998) Forest response to the introduced hemlock woolly adelgid in southern New England, USA. *Journal of the Torrey Botanical Society*, 125, 60–73.

Pearl, J.K., Anchukaitis, K.J., Pederson, N. and Donnelly, J.P. (2017) Reconstructing Northeastern United States temperatures using Atlantic white cedar tree rings. *Environmental Research Letters*, 12, 114012.

Pearl, J.K., Anchukaitis, K.J., Pederson, N. and Donnelly, J.P. (2020) Multivariate climate field reconstructions using tree rings for the northeastern United States. *Journal of Geophysical Research: Atmospheres*, 125, e2019JD031619.

Pederson, N., Cook, E.R., Jacoby, G.C., Peteet, D.M. and Griffin, K. L. (2004) The influence of winter temperatures on the annual radial growth of six northern range margin tree species. *Dendrochronologia*, 22, 7–29.

Petris, G. (2010) dlm: Bayesian and likelihood analysis of dynamic linear models. *R package version*, 1.

Roberts, S.W., Tankersley, R. and Orvis, K.H. (2009) Assessing the potential impacts to riparian ecosystems resulting from hemlock mortality in great smoky mountains national park. *Environmental Management*, 44, 335–345.

Rydval, M., Larsson, L.-Å., McGlynn, L., Gunnarson, B.E., Loader, N.J., Young, G.H. and Wilson, R. (2014) Blue intensity for dendroclimatology: should we have the blues? Experiments from Scotland. *Dendrochronologia*, 32, 191–204.

Saladyga, T. and Maxwell, R.S. (2015) Temporal variability in climate response of eastern hemlock in the central Appalachian region. *Southeastern Geographer*, 55, 143–163.

Schweingruber, F., Briffa, K. and Nogler, P. (1993) A tree-ring densitometric transect from Alaska to Labrador. *International Journal of Biometeorology*, 37, 151–169.

Schweingruber, F.H. and Briffa, K.R. (1996) Tree-ring density networks for climate reconstruction. In: *Climatic Variations and Forcing Mechanisms of the Last 2000Years*. New York: Springer, pp. 43–66.

Sheppard, P.R., Graumlich, L.J. and Conkey, L.E. (1996) Reflected-light image analysis of conifer tree rings for reconstructing climate. *The Holocene*, 6, 62–68.

Speer, J.H. (2010) *Fundamentals of Tree-Ring Research*. Tucson: University of Arizona Press.

Tardif, J., Brisson, J. and Bergeron, Y. (2001) Dendroclimatic analysis of *Acer saccharum*, Fagus grandifolia, and *Tsuga canadensis* from an old-growth forest, southwestern Quebec. *Canadian Journal of Forest Research*, 31, 1491–1501.

Trouet, V. and Van Oldenborgh, G.J. (2013) Knmi climate explorer: a web-based research tool for high-resolution paleoclimatology. *Tree-Ring Research*, 69, 3–14.

Visser, H., Büntgen, U., D'Arrigo, R. and Petersen, A. (2010) Detecting instabilities in tree-ring proxy calibration. *Climate of the Past*, 6, 367–377.

Vose, J.M., Wear, D.N., Mayfield, A.E. and Nelson, C.D. (2013) Hemlock woolly adelgid in the southern Appalachians: control strategies, ecological impacts, and potential management responses. *Forest Ecology and Management*, 291, 209–219.

Wahl, E.R. and Ammann, C.M. (2007) Robustness of the Mann, Bradley, Hughes reconstruction of northern hemisphere surface temperatures: examination of criticisms based on the nature and processing of proxy climate evidence. *Climatic Change*, 85, 33–69.

Wason, J.W. and Dovciak, M. (2017) Tree demography suggests multiple directions and drivers for species range shifts in mountains of northeastern United States. *Global Change Biology*, 23, 3335–3347.

White, P.B., Soulé, P. and van de Gevel, S. (2014) Impacts of human disturbance on the temporal stability of climate–growth relationships in a red spruce forest, southern Appalachian mountains, USA. *Dendrochronologia*, 32, 71–77.

White, P.B., Van de Gevel, S.L. and Soulé, P.T. (2012) Succession and disturbance in an endangered red spruce-fraser fir forest in the southern Appalachian mountains, North Carolina, USA. *Endangered Species Research*, 18, 17–25.

Wiles, G.C., Charlton, J., Wilson, R.J., D'Arrigo, R.D., Buma, B., Krapek, J., Gaglioti, B.V., Wiesenberg, N. and Oelkers, R. (2019) Yellow-cedar blue intensity tree-ring chronologies as records of climate in Juneau, Alaska, USA. *Canadian Journal of Forest Research*, 49, 1483–1492.

Wilson, R., Anchukaitis, K., Andreu-Hayles, L., Cook, E., D'Arrigo, R., Davi, N., Haberbauer, L., Krusic, P., Luckman, B., Morimoto, D., Oelkers, R., Wiles, G. and Wood, C. (2019) Improved dendroclimatic calibration using blue intensity in the southern Yukon. *The Holocene*, 29, 1817–1830.

Wilson, R., Anchukaitis, K., Briffa, K.R., Büntgen, U., Cook, E., D'arrigo, R., Davi, N., Esper, J., Frank, D., Gunnarson, B., Hegerl, G., Helama, S., Klesse, S., Krusic, P., Linderholm, H., Myglan, V., Osborn, T., Rydval, M., Schneider, L., Schurer, A., Wiles, G., Zhang, P. and Zorita, E. (2016) Last millennium northern hemisphere summer temperatures from tree rings: part i: the long term context. *Quaternary Science Reviews*, 134, 1–18.

Wilson, R., D'Arrigo, R., Andreu-Hayles, L., Oelkers, R., Wiles, G., Anchukaitis, K. and Davi, N. (2017a) Experiments based on blue intensity for reconstructing north pacific temperatures along the gulf of Alaska. *Climate of the Past*, 13, 1007–1022.

Wilson, R., D'Arrigo, R.D., Buckley, B.M., Büntgen, U., Esper, J., Frank, D., Luckman, B., Payette, S., Vose, R. and Youngblut, D. (2007) A matter of divergence: tracking recent warming at hemispheric scales using tree ring data. *Journal of Geophysical Research*, 112, 1–17.

Wilson, R., Rao, R., Rydval, M., Wood, C., Larsson, L.-Å. and Luckman, B.H. (2014) Blue intensity for dendroclimatology: the BC blues: a case study from British Columbia, Canada. *The Holocene*, 24, 1428–1438.

Wilson, R., Wilson, D., Rydval, M., Crone, A., Büntgen, U., Clark, S., Ehmer, J., Forbes, E., Fuentes, M., Gunnarson, B.E., Linderholm, H.W., Nicolussi, K., Wood, C. and Mills, C. (2017b) Facilitating tree-ring dating of historic conifer timbers using blue intensity. *Journal of Archaeological Science*, 78, 99–111.

Wilson, R.J. and Luckman, B.H. (2003) Dendroclimatic reconstruction of maximum summer temperatures from upper treeline sites in interior British Columbia, Canada. *The Holocene*, 13, 851–861.

Zang, C. and Biondi, F. (2015) Treeclim: an R package for the numerical calibration of proxy-climate relationships. *Ecography*, 38, 431–436.

SUPPORTING INFORMATION

Additional supporting information may be found online in the Supporting Information section at the end of this article.

How to cite this article: Harley GL, Heeter KJ, Maxwell JT, *et al.* Towards broad-scale temperature reconstructions for Eastern North America using blue light intensity from tree rings. *Int J Climatol*. 2021;41 (Suppl. 1):E3142–E3159. https://doi.org/10.1002/joc.6910